ACADEMIA ROMÂNĂ
Revue Roumaine de Chimie
http://web.icf.ro/rrch/

Rev. Roum. Chim.,
2011, *56*(10-11), 1039-1046

SYNTHESIS AND CHARACTERIZATION OF SOME COMPOSITES BASED ON NANOSTRUCTURED PHOSPHATES, COLLAGEN AND CHITOSAN

Gheorghe TOMOAIA,[a] Maria TOMOAIA-COTISEL,[b,*] Lacrimioara-Bianca POP,[b] Alexandru POP,[b] Ossi HOROVITZ,[b] Aurora MOCANU[b], Nicolae JUMATE[c] and Liviu-Dorel BOBOS[b]

[a]Iuliu Hatieganu University of Medicine and Pharmacy, Orthophaedics and Traumatology Department, 47 Traian Mosoiu Str., 400132 Cluj-Napoca, Roumania
[b]Babes-Bolyai University, Faculty of Chemistry and Chemical Engineering, 11 Arany J. Str., 400028 Cluj-Napoca, Roumania
[c]Technical University of Cluj-Napoca, Faculty of Material Science and Engineering, 103 Muncii Bd., 400641, Cluj-Napoca, Roumania

Received June 4, 2010

Nanostructured phosphates, such as hydroxyapatite (HAP) with or without various silicon (Si) contents, of controlled porosity and crystallinity as well as composite biomaterials formed of HAP powders, collagen type I (COL), and chitosan (CHI) were prepared by precipitation method and characterized *in vitro*. The HAP powders and the resulted composite biomaterials were visualized using TEM, SEM and AFM. The morphology and particle size were revealed and the influence of Si content and of synthesis conditions on the material properties were assessed. The incorporation of nanoHAP powder within collagen and chitosan matrix leads to biocomposites with good bioactivity that can be controlled by the HAP/CHI/COL weight ratios, as it was preliminary tested in cell culture.

INTRODUCTION

There is a continuous need worldwide for bone substitutes due to severe bone injuries, reconstructive surgery and degenerative diseases.[1] On this direction, the use of calcium phosphates (CP),[1-4] such as hydroxyapatite ($Ca_{10}(PO_4)_6(OH)_2$: HAP, with a Ca/P ratio of 1.67), particularly in bone reconstruction is known since 1920. The HAP properties, including biocompatibility, bioactivity and absorbing ability are greatly influenced by its morphology and grain size.[2] In this relationship, it is of great importance to develop novel HAP synthesis routes to control the morphology and grain size.

Previous work has reported that hydroxyapatite,[2-4] one of the well known calcium phosphates, due to its chemical composition and morphological similarity to natural bone mineral[5] and to its high cytocompatibility, can be used in covering metal implants, in synthesis of polymeric composites[7] and as a main component for bone cement.[8] Nevertheless, synthetic hydroxyapatite is believed to somehow mimic the natural bone properties.[9, 10]

Other compounds have been used to assist hydroxyapatite and to enhance its bioactivity. For instance, there are many attempts[11-19] to modify hydroxyapatite in order to produce composites with improved biological properties. Practically, the hydroxyapatite is partially substituted with SiO_4^{4-}, CO_3^{2-} ions for the PO_4^{3-} ions. Generally, the substitution of PO_4^{3-} ions by CO_3^{2-} or OH^- can give various kinds of substituted hydroxyapatites,[14, 15] with structure, chemical and biochemical properties more similar to the hydroxyapatite from natural bones.

Cristallinity is another main factor in bone formation and mineralization,[16, 17] which can be modified significantly by the partial substitution of PO_4^{3-} ions by SiO_4^{4-} ions.[18-25] Silicon introduced in hydroxyapatite structure allows a specific morphological structure (high porosity) and participates in biological body processes.[20, 21]

* Corresponding author: mcotisel@chem.ubbcluj.ro

The silicon in hydroxyapatite appears both in siloxanic groups (-Si-O-Si-) and in silanolic ones (-Si-OH). Silicon is also important in the manufacturing process of nanostructured hydroxyapatite, because by its adsorption at the surface of hydroxyapatite nuclei the nucleation process is accelerated, and in consequence it activates this step of nucleation against the growing step of nuclei.

In spite of all these positive aspects of hydroxyapatite, by comparing it with the inorganic constituents of natural bone some differences, both in chemical composition and morphology still exist. In addition, bone in living tissue constantly undergoes a coupled resorption-reparative process known as bone remodeling. Composites of HAP and collagen[26, 27] are recognized to induce bone growth into a porous structure and can regenerate bones and joints.

However, a gap remains to be filled because no synthetic material used up to now presents biological characteristics and medical requirements resembling to the natural bone tissue. At the present, autografts and allografts stay the standards for bone repairs, having the important advantage supporting osteogenic differentiation of marrow stromal cells (MS cells) and being osteoinductive. These systems suffer from a limited availability that keeps the high interest to develop synthetic alternative biomaterials for bone replacement. Thus, the research continues in order to obtain biomaterials, having hydroxyapatite in their composition,[1] with superior properties and increased biocompatibility and absorption rate.

The main goal of this study is to develop a new procedure to obtain nanostructured HAP, pure (nanoHAP) or with different silicon contents (nanoHAP-Si), of high crystallinity and porosity. In addition, some composites of nanoHAP with collagen, nanoHAP-Si, chitosan and collagen were obtained by deposition layer by layer technique. These composites were characterized by TEM, SEM, AFM, and X-ray diffractions.

RESULTS AND DISCUSSION

The obtained composites, namely nanoHAP, nanoHAP with 1%SiO_2 and 3% SiO_2 were characterized by X-ray diffraction, TEM, SEM and AFM.

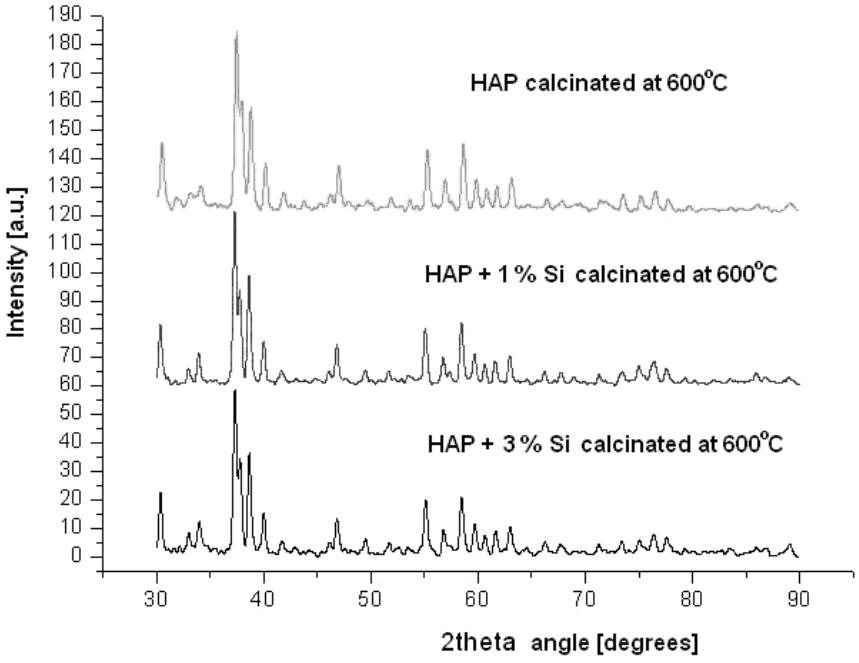

Fig. 1 – X-ray diffraction spectra for the samples of HAP, HAP + 1% Si and HAP + 3 % Si.

From the analysis of diffraction spectra (Fig. 1), it follows that both nanoHAP and nanoHAP with 1% or 3 % Si content present practically the same nanocrystalline structure. Thus, for low Si content, a single phase nanoHAP powder with or without Si can be easily obtained using our synthesis procedure (see Experimental section). After the thermal treatment (calcination), the degree of crystallinity is high.

The specific surface area and porosity of nanoHAP and NanoHAP with 1% Si or with 3% Si powders were measured by BET method using a surface analizer (Qsurf Series) and the effect of Si content and of the calcination temperature was determined (unpublished results). Briefly, the specific surface area and porosity are increased by increasing Si contents, and decreased with temperature. The samples were further imaged at the transmission electron microscope (TEM).

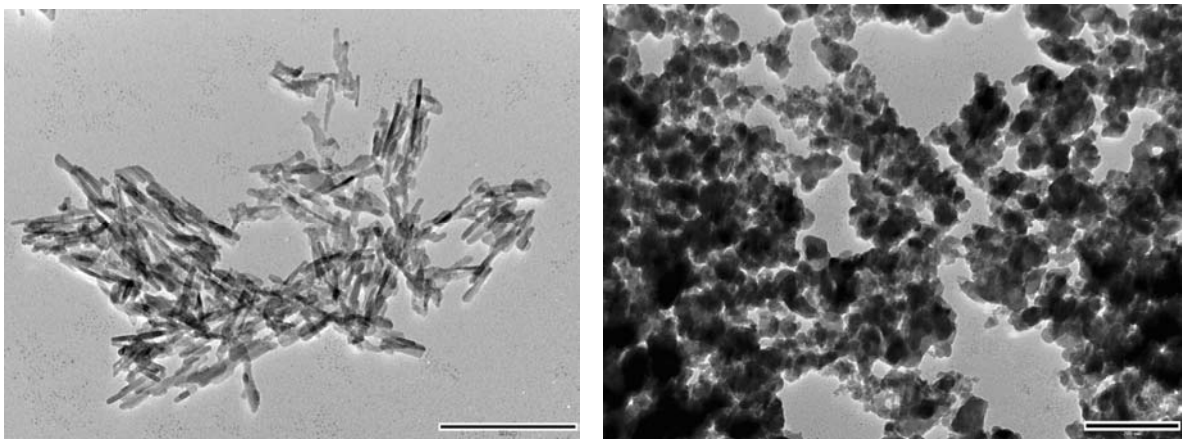

a. b.

Fig. 2 – TEM images for nanoHAP (a) and for nanoHAP with 1% Si (b); the bars in the TEM images correspond to 200 nm.

Fig. 2a shows the TEM image for HAP nanocrystals, which possess the expected needle shape. In the nanoHAP modified with Si, from Fig. 2b, it is observed that the morphology is changed from needle-like to almost spherical granules. Further, it may be seen that (a) HAP particles without Si have acicular form, (specific morphology for nanoHAP), with small particles with diameters of 7-15 nm and a length up to 100 nm, while nanoHAP-Si particles obtained by precipitation in presence of sodium silicate (b) present a spherical morphology and small sizes of 20-30 nm. More specific, the size distribution for nanoHAP-Si powder can be seen in Fig. 3.

From the histogram (Fig. 3), it appears that there is a majority of low-sized nanoparticles, but a small fraction of large particles is also observed. The average size of the nanoparticles is 17.6 nm, with a standard deviation of 23.3 nm (diameters between 2 and 130 nm). By a more detailed analysis, two populations can be discerned, one of smaller particles (between 2 and 10 nm, average size 2.9 nm, with the standard deviation of about 1.7 nm) and another one of larger particles (between 20 and 130 nm, mean: 35 nm, standard deviation: 25 nm).

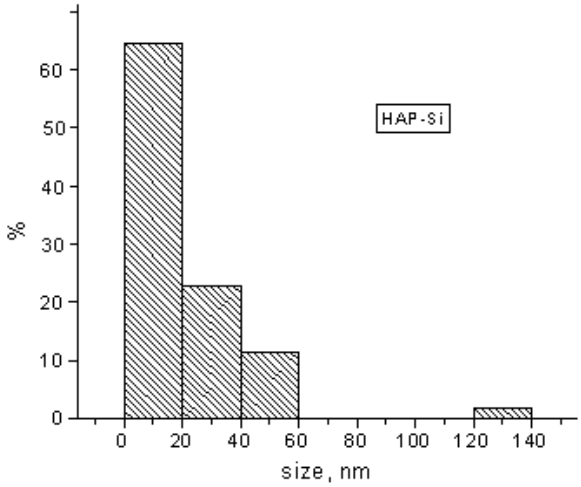

Fig. 3 – The histogram of particles of NanoHAP-Si (1%) content.

Fig. 4 shows the TEM images for self-assemblies realized within the mixed colloidal dispersion, made of nanoHAP and collagen, at a bulk weight ratio of nanoHAP:COL of 2:1. It is to be observed the mineralized collagen fibers in form of nanorods rather long above 100 nm. The darker granules indicate nanoHAP particles within the collagen fibers. The COL fibers are mineralized in aqueous dispersions of nanoHAP.

From SEM images of HAP particles, such as those presented in Fig. 5, their granulometry could be assessed and it is represented in Fig. 7a; the particles have diameters under 1 μm (between 100 and 930 nm), with an average diameter of 360 nm and a standard deviation of 180 nm.

The HAP particles with 1% Si are larger as identified in SEM micrographs given in Fig. 6. Their size distribution is represented in the histogram shown in Fig. 7b. The particles size is between about 0.6 and 41 μm, with a mean value of about 10 μm and a standard deviation of 9 μm.

Comparing the particles size in Figs. 2-7, it is to be noted that within the self-assemblies obtained by adsorption from dispersion on TEM grid support, the particles of nanoHAP (Fig. 2a) are smaller than those with Si content (Figs. 2b and 3). On the other hand, the powder particles observed by SEM (Figs. 5-7) are much larger than those in Fig. 2. This effect is due to the aggregation of particles of nanoHAP with or without Si content during the drying process of powders, and thus we can monitor the size of particles on the solid support for developing scaffolds for cell cultures. In the presence of collagen in aqueous nanoHAP dispersion, the nanoHAP particles size is not significantly modified (Fig. 4) within the collagen supramolecular associations. Therefore, the granulation and the porosity of layers of nanoHAP deposited or adsorbed on solid support can be controlled and a relationship with the adhesion, proliferation and growth of cells can be deduced and optimized (unpublished results).

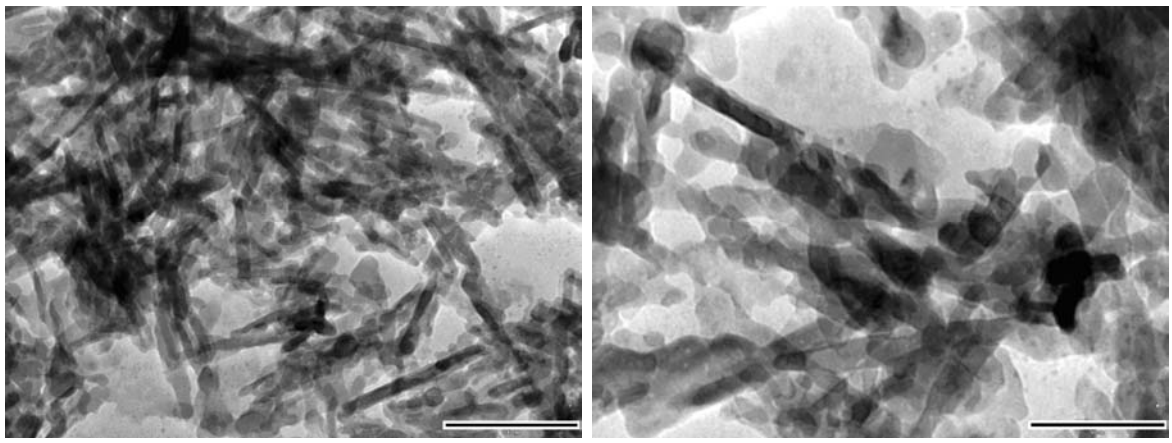

a. b.

Fig. 4 – TEM images for nanoHAP and collagen self assembly, adsorbed on TEM grids from the mixed colloidal dispersion of nanoHAP and collagen, at a weight ratio of 2:1, for two different magnifications; the bars correspond to 100 nm (a) and 50 nm (b).

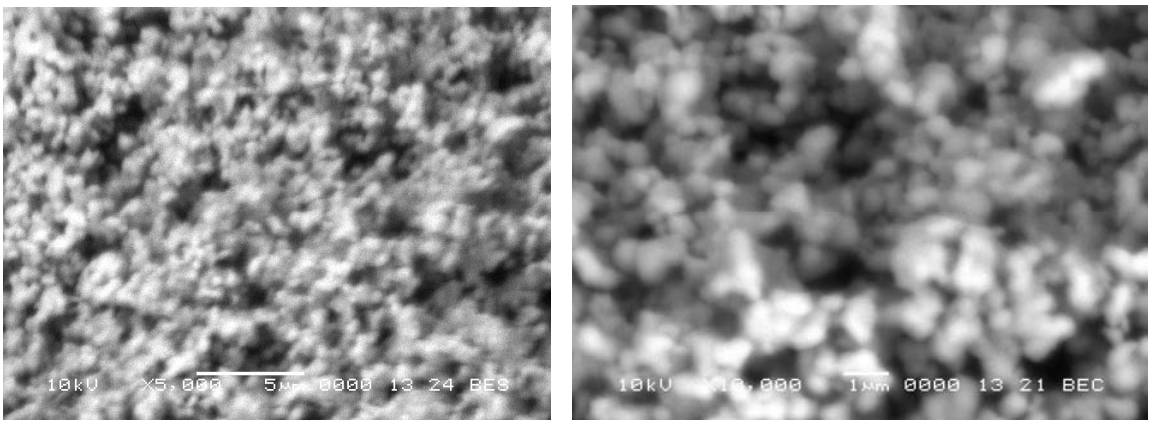

a. b.

Fig. 5 – SEM micrographs of nanoHAP self-assembled from colloidal dispersions on hydrophilic glass for two magnifications; bars correspond to 5 μm (a) and to 1 μm (b).

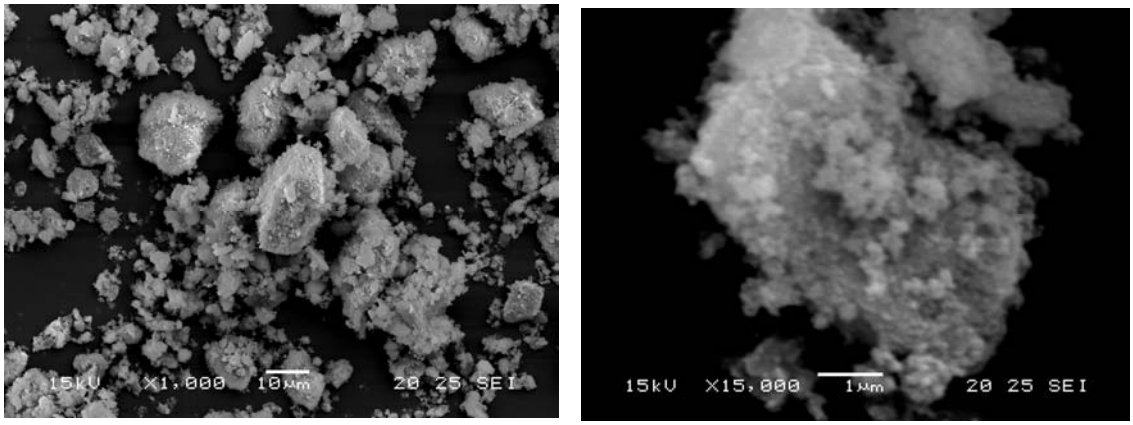

a. b.

Fig. 6 – SEM micrographs of nanoHAP-Si content (1%) self-assembled from colloidal dispersions on hydrophilic glass for two magnifications; bars correspond to 10 µm (a) and to 1 µm (b).

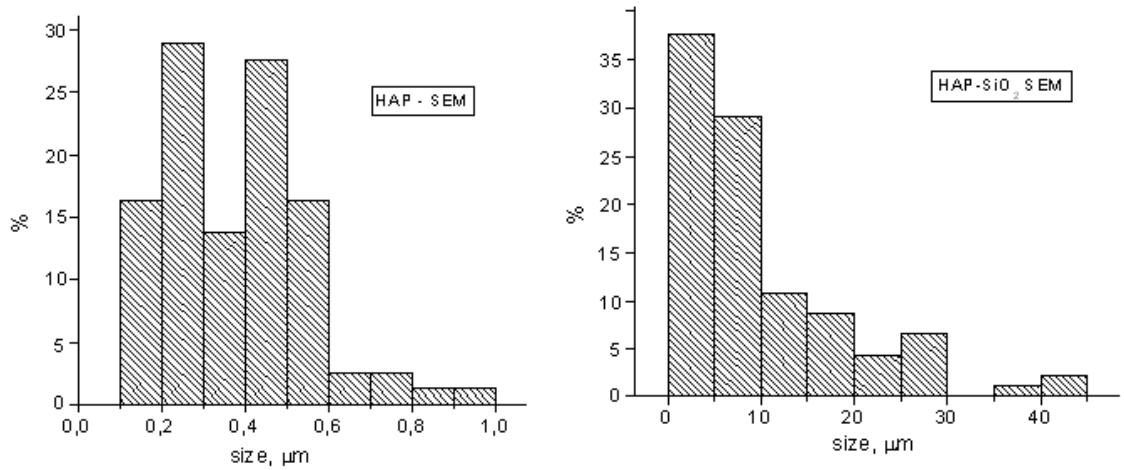

Fig. 7 – The histogram of particles of nanoHAP (a) and of nanoHAP-Si (1%) content.

Further, the nanoHAP+1% Si/chitosan/collagen (nanoHAP-Si/CHI/COL) composite was prepared using layer by layer deposition method and investigated using atomic force microscopy (AFM). The surface of this composite was imaged at room temperature (about 22 ^{o}C) and under ambient laboratory conditions as previously reported.[28-31]

The AFM images were recorded at least at six macroscopically different locations on the composite surface, with each of the locations separated by at least 10 µm. As an example, the AFM images are shown in Fig. 8, where the collagen fibers are observed on the surface of the nanoHAP-Si/CHI/COL composite (Figs. 8a-d).

The collagen fibers are arranged parallel or in different directions as mainly illustrated in Figs. 8a and 8c. In phase image (Fig. 8b), it is not easy to distinguish individual collagen fibers because the borders between fibers are somehow hidden due to the fact that some fibers are at different levels in comparison with the composite surface, visualized by AFM. The collagen fibers are rather large up to 1 µm as illustrated in the cross section profile, given in Fig. 8e.

These results support the idea that the collagen molecules are self-assembled in long (more than 10 µm) fibers that interact with chitosan layer attached to the nanoHAP-Si layer. The data are in substantial agreement with the general theory that the silicon or silicates have the capacity for adsorbing/binding organic molecules, such as chitosan and collagen ones, and aligning them on the composite surface.

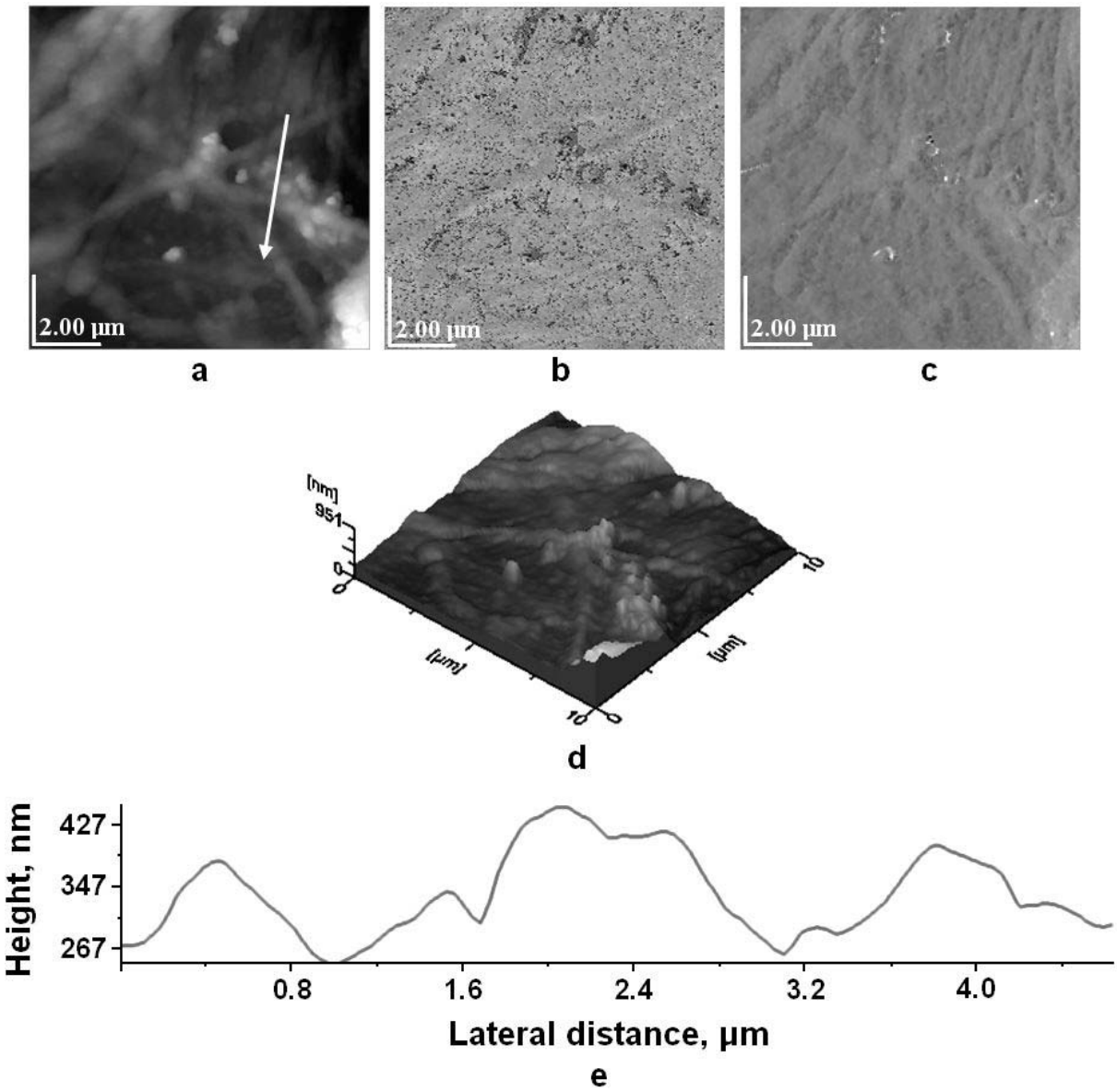

Fig. 8 – AFM images of the composite composed of hydroxyapatite, chitosan and collagen; scanned area: 10 µm x 10 µm; a) topography image, b) phase image, c) amplitude image, d) 3D view of topography, e) cross section along the arrow in panel a.

The driving force of the self-organization of chitosan or collagen with nanoHAP-Si is assumed to be the interaction between their surfaces. For instance, the interfacial interaction between Ca^{2+} ions on the nanoHAP –Si crystals and dissociated carboxyl residues on the collagen molecules might be considered. The adsorption of biomolecules, such as chitosan and collagen, on nanoHAP-Si can be probably described by hydrogen bonds, electrostatic and van der Waals forces.

EXPERIMENTAL

Materials. The starting compounds used in this work include calcium nitrate, $Ca(NO_3)_2{\cdot}4H_2O$, calcium acetate $Ca(CH_3COO)_2{\cdot}2H_2O$, diammonium hydrogen phosphate, $(NH_4)_2HPO_4$, ammonium hydroxide (NH_4OH), sodium silicate in the molar ratio of $Na_2O{:}SiO_2$ = 1:3.2, nonylphenol and acetic acid (CH_3 COOH). They were acquired from Merck. Bovine Achilles tendon collagen, type 1, was purchased from Sigma. Chitosan of medium molecular weight was obtained from Aldrich. All compounds were used without further purification. Deionized ultrapure water was used in all experiments. Collagen and chitosan were independently dispersed in deionized water at a pH of about 3, made with acetic acid (CH_3 COOH).

Synthesis of nanoHAP. Nanostructured hydroxyapatite (nanoHAP) was prepared by the synthesis procedure shown below. The $Ca(NO_3)_2 \cdot 4H_2O$ was completely dissolved in water to give 250 mL aqueous solution, noted A, having a concentration between 0.15 M and 0.24 M, and in the presence of 0.25 mL nonylphenol, at pH 6.3. Separately, $(NH_4)_2HPO_4$ was dissolved in water at a concentration between 0.036 and

0.090 M, forming 250mL of solution B, to which 45 mL of solution of 25 % NH_4OH, and 0.25 mL nonylphenol were previously added, pH = 11.5.

The two solutions A and B were mixed and the pH of the resulted colloidal dispersion was adjusted a a value between 9.5 and 11.5, with ammonium hydroxide. Then, the colloidal dispersion was sealed in a container and kept inside of a water bath for 48 hrs at 80 ^oC up to 85 ^oC for its maturation. During the maturation process, the dispersion was vigorously and continuously stirred, to allow the calcium phosphate precursors to HAP to nucleate and grow. In the presence of a surfactant, such as nonylphenol, the nucleation and the growth of nuclei can be controlled.

The presence of OH^- ions in aqueous dispersion will cause the transformation from HPO_4^{2-} to PO_4^{3-}. Therefore, the transforming process from calcium phosphate precursors to HAP was conducted and controlled by adjusting the pH of the colloidal dispersion, by adding 25 % NH_4OH solution. The resulted final suspension was filtered, and the precipitate was washed with deionized water until no NO_3^- ions were detected. Then, the precipitate was dried in supercritical conditions at -80 ^oC, under a pressure of 5 x 10^{-3} torr, and then calcinated at about 600 ^oC. The used hydrothermal method resulted in a nanostructured HAP powder of controlled stoechiometry, high cristallinity, and low sized particles.

Synthesis of nanoHAP-Si. Nanostructured silicon substituted hydroxyapatites, nanoHAP-Si, were prepared by a synthesis procedure similar with that presented above, for the preparation of nanoHAP. In addition, sodium silicate in the molar ratio, $Na_2O:SiO_2$ = 1:3.2, was added from the beginning to the diammonium hydrogen phosphate solution, noted B, in two different quantities, one for the nanoHAP-Si, with 1% Si content, and the second one for the 3% Si content into substituted nanoHAP.

The precipitation was achieved by adding, under energetic stirring, the $Ca(NO_3)_2$ solution, A, into the $(NH_4)_2HPO_4$ solution, B, after previously adding the silicate solution to B. The colloidal dispersion was further stirred continuously at a temperature between 80 and 85°C for 48 hours, for maturation. Finally, the precipitate was separated by filtering, washed with deionized water until no NO_3^- ions were detected, and dried in supercritical conditions -80°C under a pressure of p = 5x10^{-3} torr. Then, it was calcinated at 600°C.

Preparation of mixed nanoHAP and collagen dispersion. NanoHAP powder is redispersed at a wanted concentration in deionized water and the resulted colloidal dispersion is further used both for TEM investigations and for the preparation of biocomposites with collagen.

Specifically, a colloidal aqueous dispersion of collagen, type 1, COL, is prepared at pH 3, realized with acetic acid. Then, the nanoHAP dispersion was mixed with collagen dispersion and the pH was adjusted to a value higher than 4.5 to assure a good stability of HAP nanoparticles.

Preparation of nanoHAP-Si/CHI/COL. The mixed biocomposite made of nanoHAP-Si (1%), chitosan (CHI) and collagen (COL): nanoHAP-Si/CHI/COL was prepared by deposition method. The chitosan colloidal solution was prepared in acidic water at pH 3. The nanoHAP-Si and collagen dispersions were prepared as above.

The optically flat glass support was first cleaned with sulphochromic acid and washed with water. Then, it was treated with 5% HCl aqueous solution for 15 min, and afterward, rinsed in deionized water for three times, next it was shortly immersed in 2% silicate solution for ten times. On this functionalized hydrophilic glass support, the layers were deposited by adsorption from colloidal dispersions. Thus, the successive layers of hydroxyapatite substituted with Si, chitosan and collagen were deposited from their colloidal solutions on glass support by vertical adsorption for 5 minutes, with washing and drying between the layer deposition.

Layer by layer were built by the adsorption from the 6% nanoHAP-1% Si dispersion (pH = 7 – 7.5) on these functionalized hydrophilic glass support. The resulted nanoHAP-Si layer was dried and then activated by treatment with silicate aqueous solutions. Then, it was dried and chitosan layer was deposited by adsorption from 2% chitosan colloidal solution by 3 immersions. Then, the chitosan layer was dried and treated with silicate solution and followed by the adsorption of collagen layer from 0.33% collagen colloidal solution (pH = 3.5). Finally, after drying, rinsing and drying again, the material was washed with 1% acetic acid solution in order to remove Na^+ ions and for the silicic acid polycondensation.

Methods. the composites thus obtained: nanoHAP, nanoHAP_Si, with 1% or 3% Si content, nanoHAP:COL; NanoHAP:CHI:COL were characterized by X-ray diffraction, TEM, SEM and AFM.

The X-rays investigations were made with a DRON-3 diffractometer, in Bragg-Brentano geometry.

The samples were imaged by the scanning electron microscope: SEM JEOL 5600 LV, the transmission electron microscope: TEM JEOL –JEM 1010 and atomic force microscope: AFM JEOL 4210, operating in tapping mode as previously described.[28-31]

CONCLUSIONS

The nanoHAP and nanoHAP with different silicon contents (1% and 3%), nanoHAP-Si, were synthesized by precipitation method and advanced processed by hydrothermal treatment to a high crystallinity, as confirmed by X-ray diffractions. In the presence of silicon the HAP crystals turned from needle-like into a rather spherical shape, as demonstrated by TEM and SEM micrographs. Composites made of nanoHAP and collagen were produced via a coprecipitation method through which a markedly different morphology was obtained, comprising fibrils of collagen with nanoHAP randomly distributed throughout the collagen self assemblies, as shown by TEM investigation. Nano-sized HAP crystals were incorporated along the collagen fibril assemblies. Composites of nanoHAP-1% Si, chitosan and collagen were prepared by self assembly and layer by layer deposition technique. The morphology of nanoHAP-Si/CHI/COL composite is dominated by the long and large collagen fibers reassembled on nanoHAP-Si previously covered by a chitosan layer. The porous nanoHAP-Si layer, deposited on the hydrophilic glass support, promotes the self

assemblies of chitosan and collagen through interfacial interactions among the functional groups of their surfaces.

In future studies, we intend to deeply evaluate the effect of nanoporous HAP, with or without silicon, HAP and collagen, as well as HAP, chitosan and collagen on osteogenic differentiation using the bone marrow derived mesenchymal stem cells.

Acknowledgments: This research was financially supported by the project 41050 within the 2nd National Program (PN2).

REFERENCES

1. A. A. P. Mansur and H. S. Mansur, *Mater. Sci. Eng. C*, **2010**, *30*, 288-294.
2. J. C. Elliott, "Structure and Chemistry of the Apatites and Other Calcium Orthophosphates", vol. 18, Elsevier, Amsterdam, 1994.
3. R. Z. LeGeros, "Calcium Phosphates in Oral Biology and Medicine", vol. 15, S. Karger AG, Basel, 1991.
4. O. V. Sinitsina, A. G. Veresov, V. I. Putlayev, Y. D. Tretyakov, A Ravaglioli and A. Krajewski, *Mendeleev Commun*., **2004**, *14*, 179-180.
5. M.Vallet-Regi and D. Arcos, *J. Mater. Chem*., **2005**, *15*, 1509-1516.
6. K. A. Gross, S. Saber-Samandari and K. S. Heemann, *J.Biomed. Mat. Research*, **2010**, *93B*, 1-8.
7. N. Patel, I. R. Gibson, S. Ke, S. M. Best and W. Bonfield, *J. Mat. Sci. Mat. Medicine*, **2001**, *12*, 181-188.
8. W. Bonfield, *J. Biomed. Eng*., **1988**, *10*, 522-526.
9. T. J. Kinnari, J. Esteban, N. Z. Martin-de-Hijas, O. Sanchez-Munoz, S. Sanchez-Salcedo, M. Colilla, M. Vallet-Regi and E. Gomez-Barrena, *J. Med. Microbiology*, **2009**, *58*, 132-137.
10. H. Demirkiran, A. Mohandas, M. Dohi, A. Fuentes, K. Nguyen and P. Aswath, *Mater. Sci. Eng.C*, **2010**, *30*, 263-272.
11. L. L. Hench, *J. Am. Ceram. Soc*., **1991**, *74*, 1487-1510.
12. S. F. Hulbert, L. L. Hench, D. Forbers and L. S. Bowman, *Ceram. Int*., **1982**, *8*, 131-140.
13. J. Zhong and D. C. Greenspan, *J. Biomed. Mater. Res.*, **2000**, *53*, 694-701.
14. H. Oonishi, L. L. Hench, J. Wilson, F. Sugihara, E. Tsuji, M. Matsuura, S. Kin, T. Yamamoto and S. Mizokawa, *J. Biomed. Mater. Res*., **2000**, *51*, 37-46.
15. C. Ergun, T. J. Webster, R. Bizios and R. H. Doremus, *J. Biomed. Mater. Res.*, **2001**, *59*, 305-311.
16. R. A. Young and P. E. Mackie, *Mater. Res. Bull*, **1980**, *15*, 17-29.
17. R. M. Wilson, J. C. Elliott and S. E. P. Dowker, *Am. Miner*., **1999**, *84*, 1406-1414.
18. E. A. P. De Maeyer, R. M. H. Verbeeck and D. E. Naessens, *Inorg. Chem*., **1993**, *32*, 5709-5714.
19. R. M. H. Verbeeck, E. A. P. De Maeyer and F. C. M. Driessens, *Inorg. Chem.*, **1995**, *34*, 2084-2088.
20. E. M. Carlisle, *Science*, **1970**, *167*, 279-280.
21. E. M. Carlisle, *Calc. Tissue Int*., **1981**, *33*, 27-34.
22. L. L. Hench and G. P. LaTorre, in "Bioceramics", vol. 5, T. Yamamuro, T. Kokubo, T. Nakamura (Eds.), Kobunshi Kankokai, Inc., Kyoto, 1992, p. 67-74.
23. C. Ohtsuki, T. Kokubo and T. Yamamuro, *J. Non-Cryst. Solids*, **1992**, *143*, 84-92.
24. D. Arcos, D. C. Greenspan and M. Vallet-Regi, *Chem. Mater*., **2002**, *14***,** 1515-1522.
25. D. Arcos, D. C. Greenspan and M. Vallet-Regi, *J. Biomed. Mater. Res*., **2003**, *65*, 344-351.
26. A.K. Lynn, T. Nakamura, N. Patel, A.E. Porter, A.C. Renouf, P.R. Laity, S.M. Best, R.E. Cameron, Y. Shimizu and W. Bonfield, *J. Biomed. Mater. Res.,* **2005**, *74A*, 447-453.
27. D. K. Dubey and V. Tomar, *J. Mech. Phys. Solids*, **2009**, *57*, 1702-1717.
28. Gh. Tomoaia, V.-D. Pop-Toader, A. Mocanu, O. Horovitz, L.-D. Bobos and M. Tomoaia-Cotisel, *Studia Univ. Babes-Bolyai, Chem*., **2007**, *52*, 137-151.
29. Gh. Tomoaia, M. Tomoaia-Cotisel, A. Mocanu, O. Horovitz, L.-D. Bobos, M. Crisan and I. Petean, *J. Optoelectron. Adv. Mater.,* **2008***, 10*, 961-964.
30. M. Tomoaia-Cotisel, C. Prejmerean, Gh. Tomoaia, A. Mocanu, M. Trif, A. Badanoiu, T. Buruiana, O. Horovitz and A. Hosu, *J. Optoelectron. Adv. Mater.,* **2008**, *10*, 937-941.
31. Gh. Tomoaia, C. Borzan, M. Crisan, A. Mocanu, O. Horovitz, L.-D. Bobos and M. Tomoaia-Cotisel, *Rev. Roum. Chim.,* **2009***, 54*, 365-374.